


Thermal analysis of phase change materials storage in solar concentrator

Sulaiman Al-Hashmi *

Sultan Qaboos University, Center for Environmental Studies and Research, Muscat, Oman, sulimans@squ.edu.om
University of Leeds, Energy Research Institute, Leeds, UK

Mingjie Chen 

Sultan Qaboos University, Water Research Center, Muscat, Oman, mingjie@squ.edu.om

Submitted: 03.03.2023

Accepted: 18.07.2023

Published: 30.09.2023



* Corresponding Author

Abstract: Thermal analysis of high-temperature phase change materials (PCM) is conducted with the consideration of a 20% void and buoyancy-driven convection in a stainless-steel capsule. The effects of the thermal expansion and the volume expansion due to phase change on the energy storage and retrieval process are explored. The used water to fill the void between two different wax paraffin and stearic acid spheres is considered as a potential PCM for concentrated solar power. The charging/discharging process into and from the capsule wall is simulated under different boundary conditions for laminar and turbulent flows. Computational models are conducted by applying an enthalpy-porosity method and volume of fluid method to calculate the transport phenomena within the PCM capsule, including an internal air void. A simplified two-dimensional model of the PCM contained within the spheres is constructed and thermal analyses are performed for the transition from solid to liquid states. Simulated charging process modes are compared with the theory. According to experiments, the temperature distributions from 40-60 mm without and with 60 mm with copper fin have different behavior. The paraffin takes less time than stearic acid for total transformation at a rate of 0.5. The size of the sphere increases over the amount of time and the phase of the sphere to complete changes as stearic acid expands more than paraffin during the transition. Inserting a rectangular fin, that is made from copper into the ball reduces the cycle time and increases output.

Keywords: Heat analysis, Phase change materials, Thermal storage

Cite this paper as: Al-Hashmi, S., & Chen, M. Thermal analysis of phase change materials storage in solar concentrator. *Journal of Energy Systems* 2023; 7(3): 302-314, DOI: 10.30521/jes.1082104

© 2023 Published by peer-reviewed open access scientific journal, JES at DergiPark (<https://dergipark.org.tr/jes>)

1. INTRODUCTION

An energy storage system with different materials widely studied over the years and the models for its usage is well established. Providing an outstanding review of these initiatives packet-bed sensible heat sources in the context, Kalbande et al, provide an excellent summary of these activities [1]. Sharma et al., and Lentswe et al., conducted an in-depth examination of solar thermal applications that can advantage from the advent of Sensible Heat Storage (SHS) technologies, economic repercussions of SHS systems are examined in this context as well as environmental [2,3]. Thermal performance was investigated experimentally for SHS-integrated solar water heaters [4,5,6]. It is high storage density and heat storage and removal capabilities at near constant temperature during processes of charging–discharging makes a thermal capacity store, based on the concept of latent heat, a viable alternative to solid-state storage (SHS). There have been a large number of studies conducted on the thermal storage performance of materials in a different way of forms, both theoretically and experimentally. Nallusamy, examined phase/change thermal storage units with spherical capsules on both a theoretical and an experimental level, resulting in the discovery of transitory thermal characteristics [7]. Merchán et al., and Onokwai et al., used a one-dimensional distinct phase formulation to analyze the transient temperature response of a packed bed of spheres containing a phase change material. A commercial-scale thermal storage model (bed-packed) with poly-propylene spheres containing paraffin wax for both energy charging and discharging recovery phases that uses air as the thermal transfer fluid was compared to the model findings achieved experimentally [8,9]. Using three different phase change materials container geometric shapes, Beemkumar et al., and Koukou et al., studied the behavior of phase change materials encapsulated salt hydrates in a domestic hot water tank heat transfer system [10,11]. In other work, spherical capsules are used for the outperformed slab and cylindrical geometries [12,13]. Thermochemical heat storage integrated with a solar thermal system was studied by Amin et al. The packed bed latent heat source technology drastically decreased the amount of the storage tank when compared to a typical storage system. It is ideally suited for intermittent hot water needs, as the LHS system uses batchwise hot water release from the TES tank [14,15]. Zhang, investigated the behavior of three kinds of paraffin composed of 60% n-tetradecane, 50% n-hexadecane, and 40% n-pentadecane [16]. Nemš and Puertas, conducted annual simulations to compare the performance of a storage tank containing PCM to that of a conventional tank devoid of PCM. The heat storage tank with and without PCM was described using a model [17]. Ozcan, investigated the procedure of charging a spherical latent heat storage (LHS) capsule using stearic acid and paraffin as PCMs in Ref. [18]. His experimental results established that paraffin capsules melt more quickly than stearic acid capsules. Thermal energy storage (TES) has a place in thermodynamic systems because of intermittent availability and continual change in solar radiation. TES increases the system's performance and thermal reliability while also reducing the gap between supply and demand by conserving energy. Therefore, it is crucial to create TES systems that are effective and affordable. However, only a small number of solar thermal plants have used TES extensively worldwide. In addition, research into the design of TES systems for various household solar applications is ongoing [18]. A popular way to cut costs is to use computational fluid dynamics, and FLUENT software appears to be used well for a variety of engineering applications [19]. Fig. 1 presents the primary solar energy thermal energy storage options. The following features can be used to characteristics energy storage [20]:

- *Depending on the capacity of storage, the medium, and the size of the system, capacity describes the amount of energy that can be held in the system,*
- *Power is a term used to describe how quickly a system's energy can be released (and recharged),*
- *Efficiency is the relationship between the energy that is supplied to the consumers and the energy that is required to operate the energy storage device. Counts the energy lost during charging and discharging cycles,*
- *Hours to months (i.e., hours, days, weeks, and months for seasonal storage) make up the storage period, which specifies how long the energy is kept in reserve,*

- The amount of time required to charge and discharge the system is defined by the charge and discharge time,
- Cost is expressed in terms of the storage system's capacity (€/kWh) or power (€/kW), and it is influenced by the equipment's lifetime, capital costs, and operating expenses (i.e., the number of cycles).

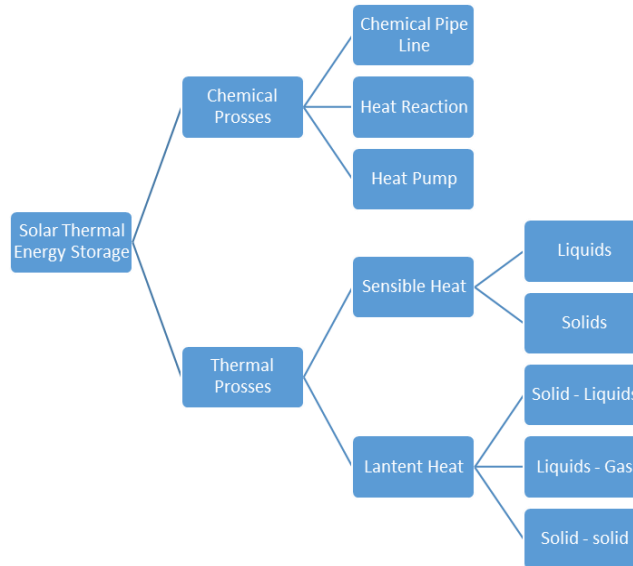


Figure 1. Solar thermal energy storage (STES) types after Ref. [2].

Power, capacity, and discharge time all depend on one another. Power and capacity may be interdependent in some storage systems. Table 1 displays typical TES system metrics such as capacity, power, efficiency, storage time, and cost. Any storage system should have high power capacity for charging and discharging as well as high-energy storage density. Three TES methods: sensible heat, PCM-related latent heat, and reaction-related thermochemical heat storage are well established to work at temperatures from -40 °C to over 400 °C (Fig. 2).

Table 1. Parameters of STES systems after Ref. [3].

STES System	Capacity (kWh /T)	Power (MW)	Efficiency (%)	Storage period	Cost (\$/kWh)
Sensible storage (Hot water)	10 -50	0.001 -10.0	50-90	Day /Months	0.1 -10
Phase change material	50 -150	0.001 - 1.0	75-90	Hours/ Months	10 -50
Chemical reactions	120 -250	1.0	75-100	Hours /Day	8 -100

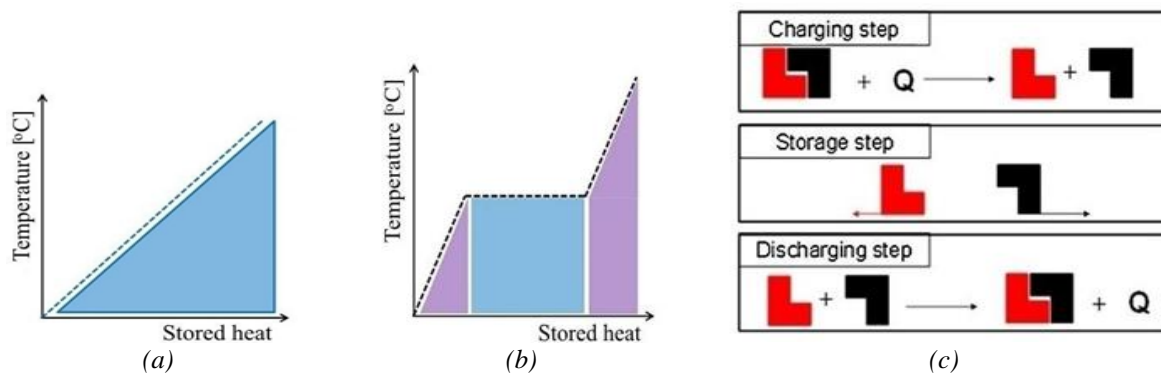


Figure 2. Three different methods of TES: (a) sensible heat storage, (b) latent heat storage and, (c) thermo-chemical reaction storage [3].

Depending on the nature of the procedure, a storage medium is chosen. Energy storage as sensible heat of stored water makes sense for water heating. Storage in sensible or latent heat effects in particle storage

units, such as sensible heat in a heat exchanger, is recommended if air-heating collectors are utilized. Storage is provided as palpable heat in the structural components of passive heating systems. If photovoltaic or photochemical processes are used, thermochemical storage makes sense.

To increase the effectiveness of latent and sensible heat thermal storage units when employed in conjunction with the constant heat source, this research intends to conduct an experimental analysis on spherical different sizes of PCM capsules (60, 50, and 40 mm). Stearic acid with paraffin is indeed the two primary components of PCMs. They are used to store and extract heat energy. Multiple diameters of PCM-filled HDPE spherical caps were employed in the TES tank, each enclosed by a material that was SHS-compliant. HTF and SHS are both made of water, where the constant temperature heat source is transferred into the TES tank. Parametric experiments are used to examine how diameter affects the installation of a copper fin.

2. SOLAR THERMAL ENERGY STORAGE

The solar thermal must be large enough to feed the power conversion system while also charging the storage system during the hours of sunlight. After sunset or during cloudy periods, thermal energy from the storage system is used to keep the engine running and generate power. When a storage system is constructed, the system's uptime can be significantly boosted, and therefore the plant's amortization can be accelerated. However, the capital commitment required is significantly greater. The first commercial projects with storage included the use of concrete or other hard base materials in the United States and Spain [14,15] PCM has many advantageous characteristics, including high volumetric storage capacities and heat availability at relatively consistent temperatures. Although energy storage systems utilizing latent heat from eutectic salts or metals have been proposed frequently, they have not been widely implemented due to challenging and expensive internal heat exchange concerns [16,17]. Solar thermal energy systems (STES) performance is primarily determined by the components that collect and store energy. Solar collectors are a form of energy exchanger that converts solar radiation into thermal energy stored in a working fluid. The most critical aspect of solar collector design and construction is optical performance, which ensures that the maximum quantity of incoming solar energy is gathered and sent to the receiver.

2.1. Sensible Heat Storage (SHS)

The presence of sensible heat produces a change in the temperature of the surrounding environment. The movement of heat from a hot to a cold environment through radiation convection as well as conduction is a property of sensible heat that distinguishes it from other types of heat.

$$Q = m C_p (T_2 - T_1) \tag{1}$$

Where m is the mass in kilograms, C_p is the heat capacity under constant pressure, and T_1 is the temperatures before and T_2 after heating, respectively. It is required to insulate this type of heat storage system to maintain a continuous temperature gradient [19].

2.2. Latent Heat Storage

In contrast to sensible heat, latent heat acts under a separate set of criteria; when heat is injected into a medium, the temperature of the material does not alter. A substance's latent heat is the energy that accumulates in increases the importance of a phase transition, and it can be defined, as the energy required to bring about a phase shift. The latent heat equation looks like this:

$$Q = m C_p \Delta T(s) + m (L + C_p \Delta T) \tag{2}$$

Where ΔT is the difference in temperature between before and after heating [20]. The sensible heat of the solid phase is the first term in the equation, followed by the latent heat of fusion and the sensible heat of the liquid phase. The specific heat of the liquid phase is the third term. When compared to other types of materials, phase-change materials have an advantage in thermal storage because of the latent heat they contain (PCMs). Because it provides a safe and convenient way of storing heat from renewable resources such as solar, as well as excess heat from industrial processes, the use of PCMs is an extremely promising technology [21]. A PCM can withstand far more heat while maintaining the same temperature as a constant-state material. As previously stated, this is due to the term latent heat. In addition to having a greater heat storage capacity, a PCM may also function as a constant temperature heat source due to its ability to gain and release heat while maintaining a constant temperature. In its phase shift state, a PCM must be able to function forever and with negligible degradation over time [22]. Among the materials that are commonly utilized, as PCMs are organic paraffin's, non-paraffin's, inorganic salts, and metallic salts and compounds. Organic paraffin's, fatty acids, or hydrates are the PCMs that are most commonly used. Even though they have all been used to capture solar or industrial waste heat, these all have melting temperatures less than 200 °C and are therefore more suitable for small-scale heating rather than large-scale power generation. When operating at high temperatures (more than 200 °C), the PCMs employed are inorganic salt, which has significantly lower thermal conductivities than organic salts, making them less effective as consistent heat sources [2,13,15,22]. The reason for phase change storage is highly effective for storage in low- temperature industrial waste and solar heat can be demonstrated with simple calculations. A paraffin wax used by Al-rawaf et al., melting point of 62°C and an enthalpy of fusion of (144-241 kJ/kg) [23]. Because water has a boiling point of 100°C, it will not undergo any change at 62°C. Therefore, water is used as a low-temperature non-PCM counterexample. With a C_p of (4.2 kJ/kg K) and an assumed starting temperature of 25°C, the sensible heat storage for water at 62°C, assuming constant specific heat, uses Eq. (1) to calculate (154 kJ/kg) [24]. When combined with the paraffin PCM's latent heat value (145-240 kJ/kg) and sensible heat, this makes the PCM beneficial at lower temperatures. PCMs start to lose their advantages at higher temperatures, for high-temperature thermal storage, molten salts and metals have latent heat values of up to (1754 kJ/kg). With operating temperatures exceeding 200°C, water converted to superheated steam, which has a heat of vaporization estimated at (2257 kJ/kg) at a temperature of 100°C. Because of this, and the fact that water has a very high heat capacity, the energy stored every kilogram of PCM is unsuitable for high-temperature heat storage.

3. EXPERIMENTAL AND METHOD

Fig. 3 shows the experimental setup of thermal model storage with different spherical sizes. In this experimental model, PCM-encapsulated sphere capsules or balls are stored in an insulating cylindrical thermal tank (TES), connecting with a flat-plate solar collector, flow meter, and circulation pump for power. Hot water for a family of five to six people can be provided by the stainless-steel tank, which is 360 mm in size and stands at 504 mm. It is necessary to ensure a consistent supply of HTF by using a flow distributor located above the tank. Glass wool is used to insulate the storage tank, which is 50 mm thick. Capsule exterior dimensions are (60, 50, and 40 mm) in diameter.

The HDPE material is used to make them with a wall thickness of 2.50 mm. To store 10,000 kilojoules of heat, a total of 152, 245, 870, 146, 235, and 836 capsules of 60, 50, and 40 mm diameter each were used in the storage tank. Wire mesh supports each layer of spherical capsules, which are arranged in a layered fashion. The melting point at paraffin is 61.2°C and the latent heat of fusion is 213 KJ/Kg. The water used to make both SHS as well as HTF is the same. With a melting point of 57.1°C and latent heat of inflection of 198 KJ/kg, the second most abundant PCM in human skin is fatty acid stearic acid.

The flow rate of HTF is monitored by a flow meter with a 2% accuracy and a centrifugal pump circulates the storage tank. Temperatures of HTF are measured at the inlet and outlet ports, as well as four segments of the tank, which are separated by ($x/L = 0.25, 0.50, 0.75, 1.01$) which, ($x/L =$ tank's dimensionless

distance from the tank's top in millimeters; x/L is the length in millimeters; x/L is the distance in millimeters less distance from the tank's top).

Each of these places has an RTD with an accuracy of around 0.3°C . To monitor the temperature for PCM, four more RTDs are inserted inside the capsules then placed and around the TES tank in four separate positions. RTDs are also depicted in Fig. 4 in terms of their position and number. In order to obtain immediate digital outputs, the RTDs are connected to a temperature meter via wire. Because of its excellent performance, spherical HDPE containers are used as PCM containers.

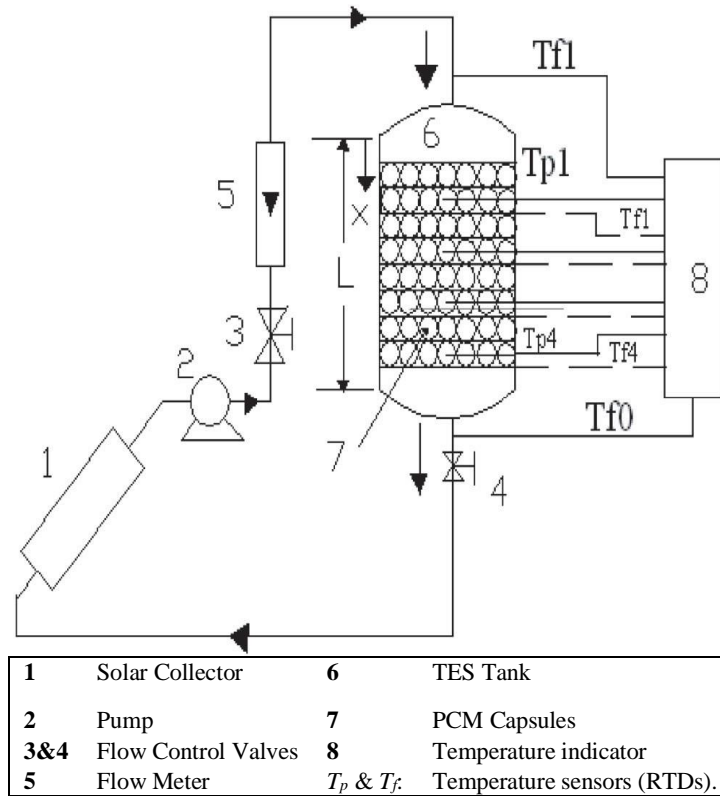


Figure 3. Experimental setup of thermal model storage with different spherical sizes.

3.1. Thermal Analysis

The thermal-transient analysis is solved using ANSYS 12 software. There were 24 parts ($N_x=24$) in the tank. One sphere is simulated for each division in the 1D model, which assumes that each portion has identical behavior. Since solids and liquids have different densities and gravitational pull, spontaneous convection occurs when PCM inside spheres changes phase.

The following presuppositions are made in this article:

- *In-compressible fluid,*
- *Density is regarded as constant except in terms of gravitational forces.*
- *Thermal and physico-chemical constants (assuming that the characteristics of the solid and liquid phases are the same).*

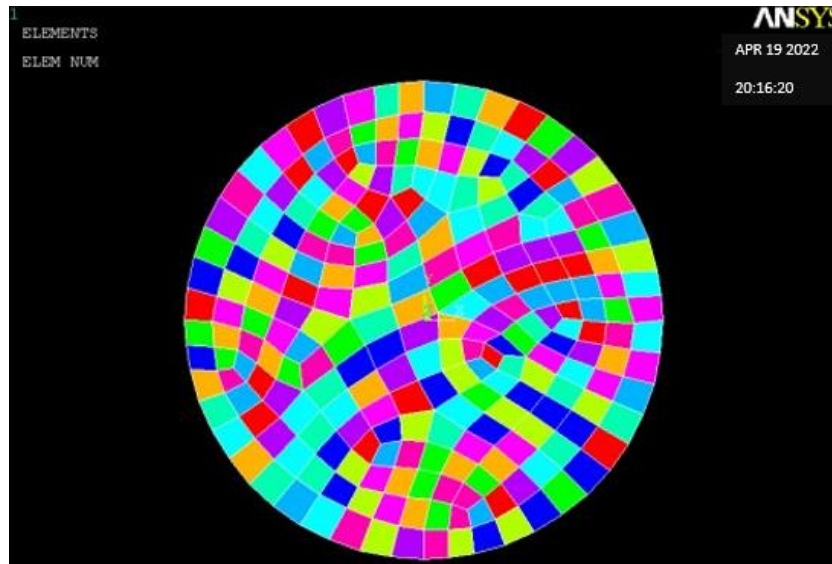


Figure 4. Meshes of PCM sphere by ANSYS software.

3.2. Results and Discussion

Fig. 5 depicts the simulation results for the thermal energy storage system's charging/discharging operation modes. The various capsule sizes utilized in the study are shown in Table 2 divided into two sections, diameter outer and diameter inner where the difference is 10 mm in each one from the other.

Table 2 The various capsule sizes which divide into two sections.

Outer Diameter (mm)	Inner Diameter (mm)
60	55
50	45
40	35

When the system is first turned on, it maintains a constant temperature of 200°C, and a water flow of 700 °C begins to enter the tank from the top when it is in charging mode. Heat transfer causes solid-state spheres to begin receiving heat and eventually melting because of this heat transfer. A representation of the flow of liquid, enthalpy (internal energy), and heat maps produced by the typical sphere in section one of the tank during power supply mode, according to ANSYS simulations and the smallest mesh taken into consideration, is shown in Fig. 5. ANSYS model with the smallest mesh taken into consideration. A solid case has been made for the existence of the phenomenon of natural convection. It is formed an ascending flow when the fluid temperature at the capsule shell is elevated over its freezing point. This ascending flow goes to and through the top of the sphere before collapsing and collapsing to meet the solid component of the capsules. A portion of the heat transferred from the solid to the liquid flow is transferred to the liquid flow, which will become cooler and falls as it passes over the solid barrier.

In this region, another ascending flow is generated, with a spinning feeling that is opposed to the spinning sense of the primary flow. This is since the temperature of the capsule at the bottom of the sphere is higher than the temperature of its interior at the top. Locally high heat transfer rates resulted from this flow, speeding up the melting process and distorting the solid part, which was originally round.

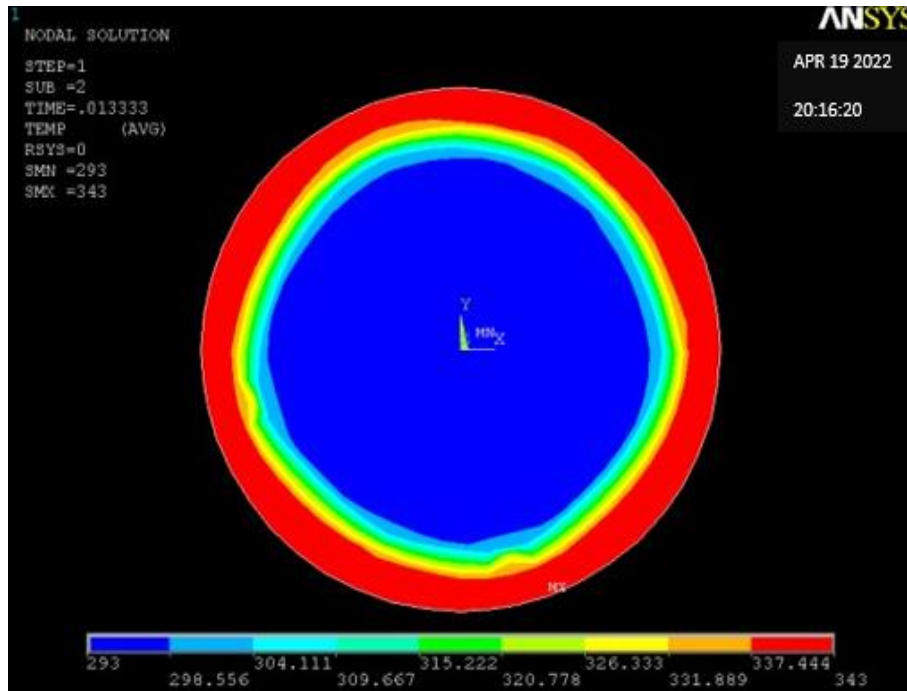


Figure 4. The temperature map of the simulated spheres by ANSYS software.

The temperature map and solid form that are produced are notably different from the concentric maps and solid forms that would normally be produced. If there were no convection, the following outcome would be obtained. It should be noted that no consideration has been given to the forces acting on the solid itself in this piece of writing. These tend to push the solid component of the capsule to the bottom of the capsule at some point during the melting process, diverging the evolution of the capsule from that predicted by our mathematical model. These ramifications should be taken into account in the creation of future products. Figures with spheres reflect the numerical findings of simulations performed on the simplified analysis for constant phase transition temperature. The numerical findings of simulations performed on the simplified analysis for constant phase transition temperature are shown in the figures. According to the simulation results at various time steps from Figs. 6(a-f), the temperature distribution inside the PCM sphere as more than just a function of the time. We recorded the time it took for different spherical diameters and PCM materials, which included paraffin wax and stearic acid, to complete a temperature distribution. The values are tallied and a comparative examination is performed.

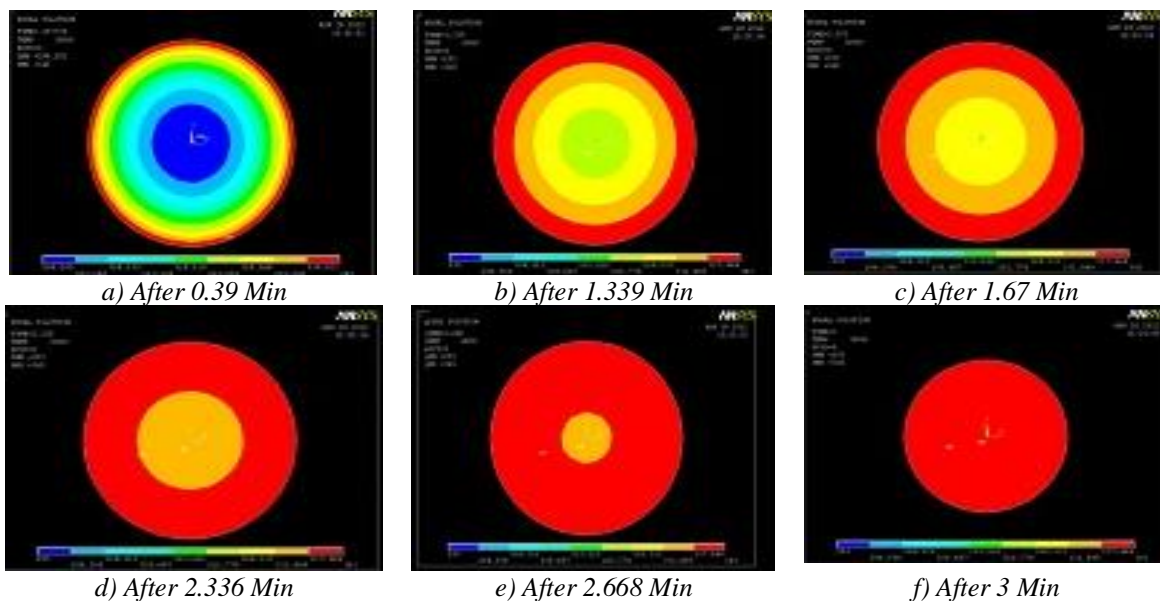


Figure 5. PCM-sphere simulation obtained at different time steps.

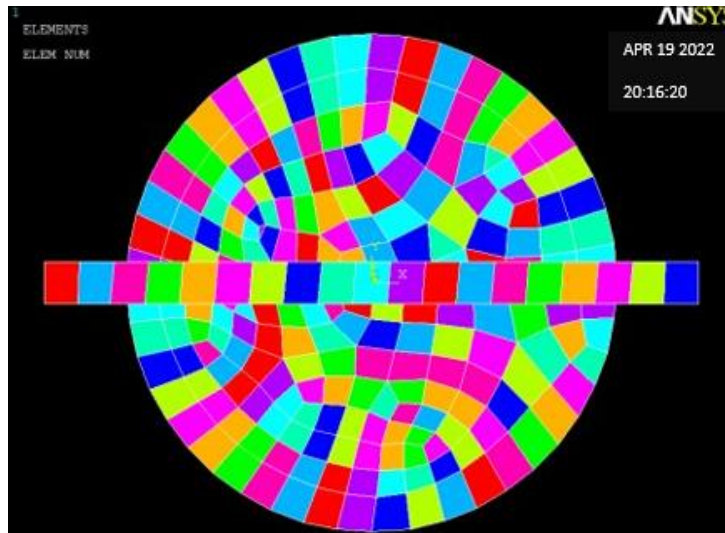


Figure 6. A PCM- sphere after a Copper fin has been introduced uses ANSYS software.

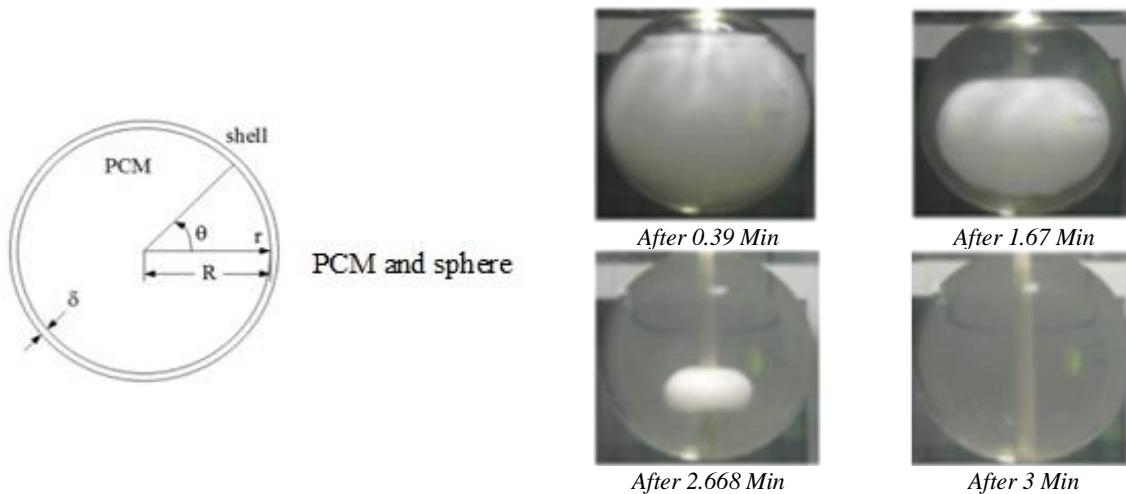


Figure 7. Comparison between paraffin wax and stearic acid in different spheres sizes and take different times to PCM's liquid specific heat capacity.

An accelerated percentage of temperature distribution in the ball is shown in Fig. 7 after a Copper fin has been added to the mesh model of the PCM sphere.

Table 3 Comparison between paraffin wax and stearic acid materials temperatures distribution from 40-60 mm without and 60 mm with copper fin.

	Sphere Size (mm)	Complete Time (Mints)	
		Paraffin wax Mints	Stearic Acid Mints
1	60	3	3.5
2	50	2	2.5
3	30	1.2	1.55
4	60-Copper fin	2.7	3.2

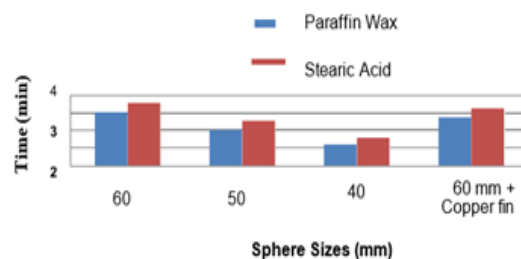


Figure 9. Comparison of PCM's liquid specific heat capacity times between paraffin wax and stearic acid in different spheres sizes (40, 50, 60 mm, and 60 mm with copper fin).

Table 3 shows the time it takes for a full phase change to occur when three different-sized spheres are compared to one another. Due to the fact, that PCM's liquid-specific heat capacity in the actual instance is larger than the values derived by mathematical calculation.

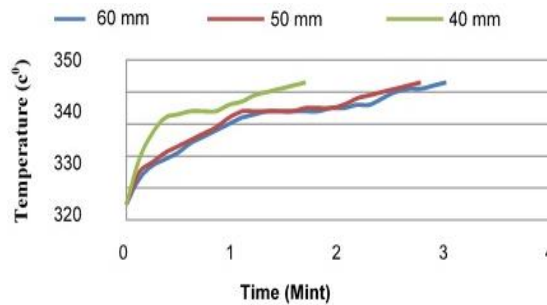


Figure 10. Temperature profiles for different spheres (40, 50, 60) mm sizes.

Following the results of the experiment, while Fig. 7 show the PCM- sphere after a Copper fin in simulation and Fig. 8 show a graph depicting the time needed to complete full phase change for spheres of various shapes and sizes, both with and without fins, as demonstrated. According to Fig. 9, the time necessary to complete the phase change in the sphere varies according to the size of the sphere, with paraffin taking less time to complete the phase shift than stearic acid in these circumstances. A rectangular cross-sectional copper fin is incorporated into the sphere and rotated radially, which significantly decreases the amount of time needed, increasing the output of various-sized balls. Fig. 10 shows that the phase shift occurs at a specific temperature in the theoretical predictions, whereas the phase shift is detected at a temperature that is close to a constant temperature as in experimental investigation. The reason is that PCMs do not have a singular melting point and melt regularly throughout a wide temperature range. The melting temperature of a paraffin wax and stearic acid mixture used as the PCM in the current experiment was previously indicated to be in the range of 590 °C to 610 °C. This is consistent with the results of the prior experiment. The temperature rise observed in the experimental results after the complete melting of PCM at any segment is lower than that predicted by the computational model.

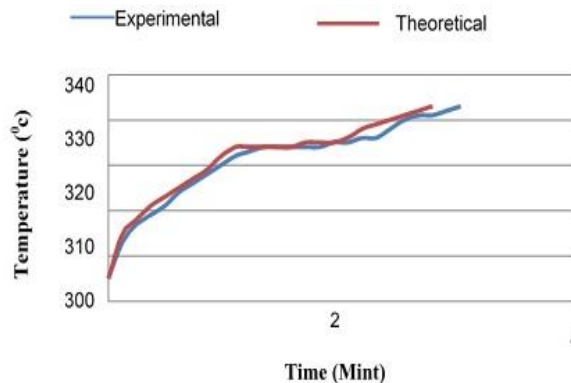


Figure 11. Comparison of the theoretical and experimental temperatures of PCM in TES tank.

A comparison of the theoretical and experimental PCM temperature histories in the TES tank can be seen in Fig. 10, which applies to the case of consistent HTF inlet temperature. Practical values are consistently lower than theoretical ones, as shown in Fig. 11, even when the temperature of the HTF intake remains constant during the charging time (see the previous section). A relatively little temperature discrepancy can be investigated by comparing theoretically and experimentally temperatures. However, in the experiment due to the limitations of the maximum temperature, that can be achieved (70 °C-73 °C) depending on the type of heat source used. It is true in the theoretical analysis because a linear increase in heat flux is observed that increases the HTF inlet temperature linearly with time is observed in the theoretical analysis (see Fig. 6). When the PCM is in a solid state, all of the numerical approaches produce numbers that are nearly equal for the temperature of the PCM during the

melting process when the PCM is in a solid state. In the first instance, when the effective heat capacity method with a wide temperature range is used, the PCM melts instantly. The melting process begins when the temperature reaches 600 °C. According to an examination of the experimental and theoretical data sets, it appears that the PCM melts a little too soon. All of the computational results for the temperature of the PCM are in great agreement with the experimental data acquired for the same temperature. When the PCM is in a liquid condition during the solidification process, all of the theoretical approaches yield uniform results for the temperature of the PCM, regardless of whatever method is employed to measure it. Upon initiation of solidification, the effective heat capacity approach, which operates over a wide temperature range, yields result that are almost equivalent to those obtained by the enthalpy method. Similar occurrences to those discovered in the store without a fin may be observed in the findings from the storage with a fin, showing that storage with a fin is more efficient. Meanwhile, while the melting process is taking place, the theoretical method yields the most precise results for PCM temperature measurements taken in the middle of the storage activity in the issue. The PCM melts too quickly on the sides of the storage container, causing the container to overflow. Another factor contributing to the disparity between theoretical and experimental results in the material properties of PCM is the assumption made in the theory that the density and heat conductivity of the PCM remains constant throughout time. The theoretical approaches will yield more precise findings for the temperature of the PCM than empirical methods, assuming that the temperature-dependent characteristics of the material are understood. It follows that the material properties of the PCM must be thoroughly known to provide conclusions that are sufficiently exact when numerical methods are used to conduct the research. One other possible explanation for the mismatch between theoretical and experimental results is that the thermocouples were not placed in the same locations in both cases. It is necessary to pour the liquid PCM into a storage container. A Possible change to the position of the thermocouple was made during the manufacturing process. Once the storage container is full, it will be hard to inspect the position of the thermocouple in any detail.

4. CONCLUSION

Utilizing the concepts of sensible and latent heat (thermal) storage strategies in conjunction with one another, it has been proven that a thermal energy storage system capable of storing hot water at an average temperature of 45 °C for household applications may be built. Charge experiments have been performed on the TES unit to evaluate its performance. These experiments have been performed using a reliable heat source that is connected to a TES unit via a specific cable. This research examines both the temperature history of HTF and PCM throughout the charging process and the energy storage capacity of HTF and PCM during the charging period, for a variety of different diameter capsules (60, 50, 40 mm) and many different types of PCMs (paraffin wax - stearic acid). A thorough understanding of the solid-to-liquid phase transition necessitates doing extensive thermal-transient analytical simulations. Several simulations of the charging mode are carried out, and the results obtained are compared with past results, leading to the conclusion that they are quite similar to experimental procedures. This study compares the results for paraffin and stearic acid, as well as different diameters of the microspheres and the presence or absence of a fin placed into the microspheres, to decide which is preferable. It has been discovered that, in some cases, the time required to complete the phase shift in the sphere varies with the size of the sphere, with paraffin needing less time than stearic acid when compared to other materials. Putting a rectangular-sectioned copper fin in the center of a ball shortens the time it takes to perform the process while simultaneously increasing the output volume. Both paraffin and stearic acid emit a similar quantity of water, with just a slight difference of 3-4 % between the two compounds in terms of water content. With as little as a 5-7 % difference in their respective values, both PCMs have comparable latent heat, heat capacity, and specific heat. However, in the market, the cost of stearic acid is roughly \$0.48/kg, and the cost of paraffin is approximately \$0.75/kg. Its economics are such that it will provide the same yield at a lower initial cost than other acids, such as acetic acid. This has led to the discovery of stearic acid as the most appropriate material for thermal energy storage systems.

Acknowledgement

The study is funded by Oman National Grant #RC/RG-DVC/WRC/21/02 and Sultan Qaboos University Grant #IG/DVC/WRC/22/02.

REFERENCES

- [1] Kalbande, VP, Fating, G, Mohan, M, Rambhad, K, Sinha, AK. Experimental and theoretical study for suitability of hybrid nano-enhanced phase change material for thermal energy storage applications. *Journal of Energy Storage* 2022; 51: 104431. DOI: 10.1016/j.est.2022.104431.
- [2] Sharma, A, Chen, CR, Murty, VVS, Shukla, A. A review of thermal energy storage designs, heat storage materials, and cooking performance of solar cookers with heat storage. *Renewable and Sustainable Energy Reviews* 2009; 13(6–7): 1599–605. DOI: 10.1016/j.rser.2008.09.020.
- [3] Lentswe, K, Mawire, A, Owusu, P, Shobo, A. A review of parabolic solar cookers with thermal energy storage. *Heliyon* 2021. 7(10): e08226. DOI: 10.1016/j.heliyon.2021.e08226.
- [4] Cruickshank, CA, Baldwin, C. Sensible Thermal Energy Storage: Diurnal and Seasonal. *Storing Energy 2016; With Special Reference to Renewable Energy Sources*: 291–311. doi 10.1016/B978-0-12-803440-8.00015-4.
- [5] Tendulkar, R, Doupis, D, Clark, M, Joshi, A, Wang, C. Transient Simulation of High-Temperature High-Pressure Solar Tower Receiver. *Energy Procedia* 2015; 69: 1451–60. doi 10.1016/j.egypro.2015.03.093.
- [6] Olsthoorn, D, Haghighat, F, Moreau, A, Joybari, MM, Robichaud, M. Integration of electrically activated concrete slab for peak shifting in a light-weight residential building—Determining key parameters. *Journal of Energy Storage* 2019; 23: 329–43. DOI: 10.1016/j.est.2019.03.023.
- [7] Nallusamy, N, Sampath, S, Velraj, R. Study on the performance of a packed bed latent heat thermal energy storage unit integrated with solar water heating system. *Journal of Zhejiang University: Science* 2006; 7(8): 1422–30. DOI: 10.1631/jzus.2006.A1422.
- [8] Merchán, RP, Santos, MJ, Medina, A, Calvo Hernández, A. High temperature central tower plants for concentrated solar power: 2021 overview. *Renewable and Sustainable Energy Reviews* 2022; 155: 111828. DOI: 10.1016/j.rser.2021.111828.
- [9] Onokwai, AO, Okonkwo, UC, Osueke, CO, Okafor, CE, Olayanju, TMA, Dahunsi, SO. Design, modelling, energy and exergy analysis of a parabolic cooker. *Renewable Energy* 2019; 142: 497–510. DOI: 10.1016/j.renene.2019.04.028.
- [10] Beemkumar, N, Karthikeyan, A. Experimental Investigation on Enhancement of Heat Transfer in Thermal Energy Storage System Using Paraffin Wax as PCM. *Applied Mechanics and Materials* 2015; 766–767: 457–462. DOI: 10.4028/www.scientific.net/amm.766-767.457.
- [11] Koukou, M, Michail, V, Pagkalos, C, Konstantaras, J. In: EinB 2018 7. International conference Energy in Buildings. Study of Heat Transfer in a Latent Heat Storage System using Salt Hydrates for Domestic Heating Applications; 3 November 2018, researchgate.net/publication/336642720 ,pp. 125-134.
- [12] Nkhonjera, L, Bello-Ochende, T, John, G, King'ondo, CK. A review of thermal energy storage designs, heat storage materials and cooking performance of solar cookers with heat storage. *Renewable and Sustainable Energy Reviews* 2017; 75: 157–67. DOI: 10.1016/j.rser.2016.10.059.
- [13] Kenisarin, MM. Thermophysical properties of some organic phase change materials for latent heat storage. A review. *Solar Energy* 2014; 107: 553–75. DOI: 10.1016/j.solener.2014.05.001.
- [14] Amin, NAM, Bruno, F, Belusko, M. Effective thermal conductivity for melting in PCM encapsulated in a sphere. *Applied Energy* 2014, 122: 280–7. DOI: 10.1016/j.apenergy.2014.01.073.
- [15] Li, W, Li, SG, Guan, S, Wang, Y, Zhang, X, Liu, X. Numerical study on melt fraction during melting of phase change material inside a sphere. *International Journal of Hydrogen Energy* 2017; 42(29): 18232–9. DOI: 10.1016/j.ijhydene.2017.04.136.
- [16] Zhang, P, Xiao, X, Ma, ZW. A review of the composite phase change materials: Fabrication, characterization, mathematical modeling and application to performance enhancement. *Applied Energy* 2016; 165: 472–510. DOI: 10.1016/j.apenergy.2015.12.043.
- [17] Nemš, A, Puertas, AM. Model for the discharging of a dual pcm heat storage tank and its experimental validation. *Energies* 2020. 13(21). DOI: 10.3390/en13215687.
- [18] Ozcan, A, Arman Kandirmaz, E. Poly[(Vinyl Alcohol) - (Stearic Acid)] Synthesis and Use in Lavender Oil Capsulation. In: 9th International Symposium on Graphic Engineering and DesignAt: Novi Sad - Serbia; 8-10 November 2018: The University of Novi Sad 189–96. DOI: 10.24867/grid-2018-p23.
- [19] Olivkar, PR, Katekar, VP, Deshmukh, SS, Palatkar, SV. Effect of sensible heat storage materials on the thermal performance of solar air heaters: State-of-the-art review. *Renewable and Sustainable Energy Reviews* 2022; 157: 112085. DOI: 10.1016/j.rser.2022.112085.
- [20] Chaatouf, D, Salhi, M, Raillani, B, Amraqui, S, Mezrhab, A, Naji, H. Parametric analysis of a sensible heat storage unit in an indirect solar dryer using computational fluid dynamics. *Journal of Energy Storage* 2022; 49: 104075. DOI: 10.1016/j.est.2022.104075.
- [21] Zvenigorodsky, S, Chudnovsky, A, Skop, H. Humidification of industrial process flows by means of waste heat recovery. In: Proceedings of the Thermal and Fluids Engineering Summer Conference; 9-12 Augus 2015: ASTFE, 1511–7. DOI: 10.1615/tfesc1.iam.012957.

- [22] Zhang, C, Li, J, Chen, Y. Improving the energy discharging performance of a latent heat storage (LHS) unit using fractal-tree-shaped fins. *Applied Energy* 2020, 259: 114102. DOI: 10.1016/j.apenergy.2019.114102.
- [23] Al-rawaf, MA, Jalil, JM. Numerical investigation of thermal performance and phase change of wax paraffin layer surrounding water tank. In: Proceeding of 15th Scientific Conference; 23-24 April 2016 ,researchgate.net/publication/316665948, pp. 19-33.
- [24] Barz, T, Sommer, A. Modeling hysteresis in the phase transition of industrial-grade solid/liquid PCM for thermal energy storages. *International Journal of Heat and Mass Transfer* 2018; 127: 701–13. DOI: 10.1016/j.ijheatmasstransfer.2018.08.032.